SLAC-PUB-2986
October 1982
(E/T)

PHYSICS WITH THE MAC DETECTOR*

Presented by D. M. Ritson

for

The MAC Collaboration

W. T. Ford, A. L. Read, Jr., and J. G. Smith

Department of Physics
University of Colorado, Boulder, Colorado 80309

A. Marini, I. Peruzzi, M. Piccolo, and F. Ronga

Laboratori Nazionali Frascati dell' I.N.F.N., Italy

L. Baksay, H. R. Band, W. L. Faissler, M. W. Gettner, G. P. Goderre, B. Gottschalk,[a] R. B. Hurst, O. A. Meyer, J. H. Moromisato, W. D. Shambroom, E. von Goeler, and Roy Weinstein

Department of Physics
Northeastern University, Boston, Massachusetts 02115

J. V. Allaby,[b] W. W. Ash, G. B. Chadwick, S. H. Clearwater, R. W. Coombes, Y. Goldschmidt-Clermont,[b] H. S. Kaye, K. H. Lau, R. E. Leedy, S. P. Leung,[c] R. L. Messner, S. J. Michalowski,[d] K. Rich, D. M. Ritson, L. J. Rosenberg, D. E. Wiser, and R. W. Zdarko

Department of Physics and Stanford Linear Accelerator Center
Stanford University, Stanford, California 94305

D. E. Groom, H. Y. Lee, and E. C. Loh

Department of Physics
University of Utah, Salt Lake City, Utah 84112

B. K. Heltsley, M. C. Delfino, J. R. Johnson, T. Maruyama, and R. Prepost

Department of Physics
University of Wisconsin, Madison, Wisconsin 53706

*Work supported in part by the U. S. Department of Energy, under contract numbers DE-AC02-76ER02114, DE-AC03-76SF00515, and DE-AC02-76ER00881, by the National Science Foundation under contract numbers NSF-PHY77-21210, NSF-PHY77-21297, and NSF-PHY5-39485.

[a]Present address: Cyclotron Laboratory, Harvard University, Cambridge, MA 02138.
[b]Present address: CERN, Geneva, Switzerland.
[c]Present address: 20 Cain Road, Hong Kong, B.C.C.
[d]Present address: Mechanical Engineering Department, Stanford University, Stanford, CA 94305.

(Presented at the XXI International Conference on High Energy Physics, Paris, July 26-31, 1982.)

Abstract

New results, obtained during the previous year at the PEP colliding beam rings with the MAC detector at a center of mass energy of 29 GeV, are presented.

Introduction

The MAC collaboration has analyzed close to all of the data obtained at the PEP colliding beam ring since switch-on. This corresponds to data, available for analyses, based on integrated luminosities of between 20 and 30 pb^{-1}. The detector combines close to full solid angle coverage with calorimetry, an inner drift detector and magnetized iron muon detection. These properties have resulted in a number of new or improved physics results, a number of which are summarized below.

1. Properties of Tau-Leptons

a. Lifetimes

Our results are based on a sample of 280 tau decays into three-charged particles. Figures 1(a) and 1(b) show the fitted event and weighted event histograms for the measured vertex decay paths. Our best lifetime value is

$$\tau_\tau = [4.1 \pm 1.1(\text{stat}) \pm 1.2(\text{sys})]\ 10^{-13}\ \text{sec} .$$

b. Tau-Branching Ratios

With an integrated luminosity of 24.8 pb^{-1}, 583 tau pairs were observed decaying into one-charged prong and three-charged prongs, respectively. This corresponded to

$$BR(\tau \to 3\text{-prong} + \text{neutrals}) = (15.3 \pm 0.7 \pm 1.0)\% .$$

118 events were found with a muon decay plus a three-charged prong decay, corresponding to

$$BR(\tau \to \mu\nu\bar{\nu}) = (17.6 \pm 1.5 \pm 1.0)\% .$$

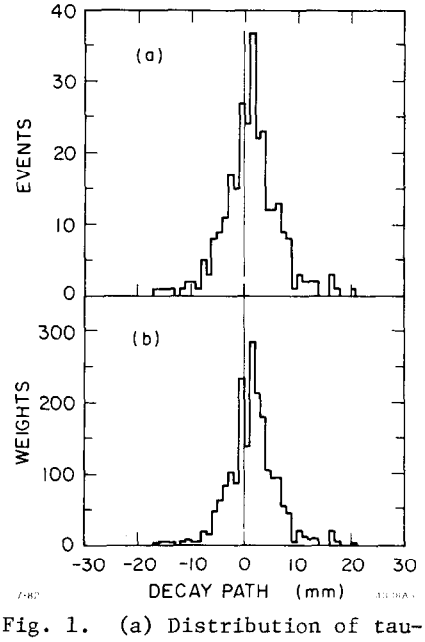

Fig. 1. (a) Distribution of tau-lepton decay paths for fitted vertices relative to the beam interaction point. (b) Distribution of decay paths for tau-leptons statistically weighted.

Only two candidates were observed to decay into a muon and a five-charged prong jet. At least one of these events was consistent with two of the charged prongs arising from a photon conversion in the beam pipe leading to

$BR(\tau \to 5\text{-prong}+\text{neutrals}) < 0.7\%$ with a 95% C.L.

2. QCD Determinations

a. Energy-Energy Correlations

Figure 2 shows the calorimetrically determined full energy-energy correlation using 97% x 4π solid-angle coverage. The data is corrected for detector biases, radiative effects and weak decays. Fitting to the perturbative QCD result to order α_s^2, a $q\bar{q}$ fragmentation term $(A_0/\sqrt{s})\sin^{-3}$, and a $q\bar{q}g$ fragmentation term $(\alpha_s A_1/\sqrt{s})$ $[\sin^{-3}\chi\ (\chi < \pi/2); \sin\chi\ (\chi > \pi/2)]$ we obtained

$$\alpha_s = 0.16 \pm 0.006(\text{stat}) \pm 0.02(\text{sys}).$$
$$A_0 = 1.20 \pm 0.080 \pm 0.15\ \text{GeV}.$$
$$A_1 = 2.5 \pm 0.20 \pm 0.4\ \text{GeV}.$$

b. R-Value for Annihilation into Multi-Hadrons

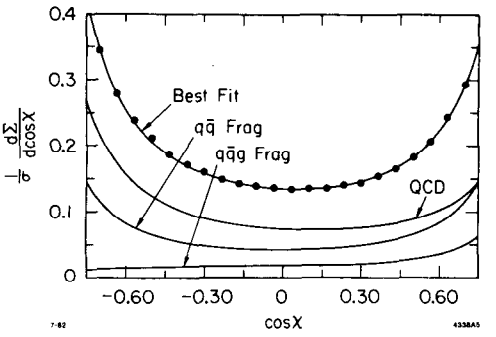

Fig. 2. The full experimental energy-energy correlation as a function of cosχ, the correlation angle. Also shown are the fitted contributions from QCD, the $q\bar{q}$ and the $q\bar{q}g$ fragmentation terms.

R was determined from two methods. The first method used nearly the full acceptance of the detector and removed two photon backgrounds with cuts on E_{vis}, $E_{\perp}$ and energy imbalance. The second method accepted only events whose thrust axis, as determined from the inner drift tracks, lay in the range 55^{o}-125^{o} to the beam axis. Figure 3 shows schematically the method used to estimate two-photon contributions to the cross section using the energy distribution histogram. The results are

Predicted

$$R = 3.67\cdot(1 + \alpha_s/\pi) \simeq 3.9$$

Observed with full-acceptance

$$R = 3.93 \pm 0.04 \pm 0.12 \pm [0.12 \text{ (radiative sys)}]$$

Observed with fiducially cut-acceptance

$$R = 3.87 \pm 0.04 \pm 0.10 \pm [0.10 \text{ (radiative sys)}]$$

Radiative corrections were made to the luminosity and multihadron cross sections to α^3 only. An estimate of the systematic errors arising from the omission of the higher order radiative terms is included in the error assignments.

3. Two Gamma Physics

a. Muon Pair Production

Figure 4 shows the distribution of two photon produced mu-mu events. The section criteria were based on acollinear muon pairs with each muon momentum greater than 1.5 GeV/c. 2,374 events were observed in 25 pb^{-1}. The data agree well with the absolute predicted Monte Carlo distribution and give

$$dN/dp_{\perp}^{2} = A\cdot p^{-i}$$

with $i = 4.02 \pm 0.50$ with a $\chi^2/df = 12.9/18$.

b. Ratio of Multihadron Events to Muon Pairs, with Electron Tags

Events were selected by requiring an isolated electron at $\geq 18^{o}$ to the beam axis and an associated electromagnetic shower in excess of 6 GeV. Muon events

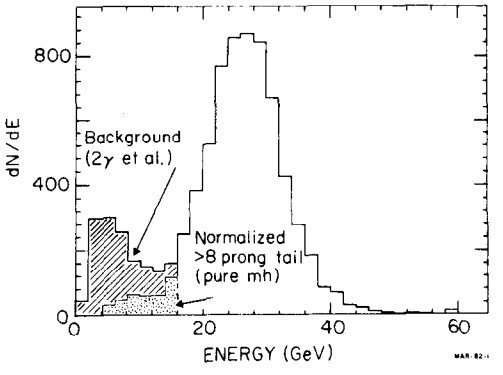

Fig. 3. The distribution of event energies, as determined from calorimetry, for events with momentum thrust-axes θ in the range 55^{o}-125^{o}. The dotted region shows the multihadron contribution for energies below 16 GeV, as estimated from the multihadron sample with > 8 prongs. The hatched area is the estimated contribution from two photon events and other backgrounds.

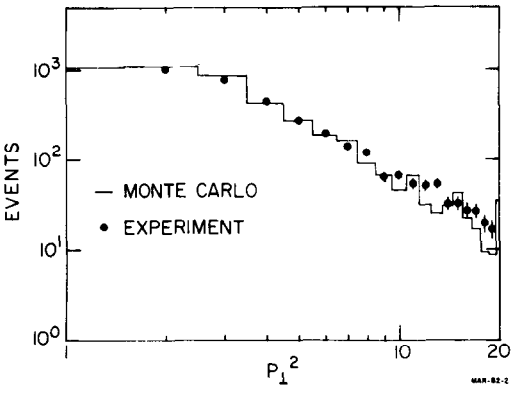

Fig. 4. The distribution of two photon produced mu-mu events as a function of $p_\perp^2$. The histrogram is the Monte Carlo prediction and shows the excellent agreement of prediction and theory.

required at least one identified muon and multihadron events ≥ 3 charged tracks. 133 eμμ and 104 e-hadron events were found in 30 pb^{-1}. 90% of the events had invariant masses > 2 GeV, and the squared four momentum transfers were in the range of 20 - 100 $(GeV/c)^2$. After subtracting backgrounds from inelastic Compton scattering (9%) and tau pairs (8%) and folding in the detection efficiencies a value of R' in terms of N_{had} and $N_{\mu\mu}$, the corrected numbers of multihadron and muon pairs, was obtained, namely,

$$R' = N_{had}/N_{\mu\mu} = 0.95 \pm 0.12 \pm 0.20$$

in good agreement with the quark model prediction of $3\Sigma e_q^4$ taking into account threshold effects for charm production.

4. Inclusive Muon Detection and Flavor Tagging

a. Particle Searches and the Inclusive Lepton Spectrum

Surrounding the MAC calorimetric detectors are four separated layers of drift counters that detect and measure angles and positions of emerging muons. Combined with the magnetized steel of the detector, these layers provide momentum and position vectors for detected muons. Restricting muon momenta to values ≥ 2 GeV/c reduced the backgrounds from punch-through processes to low levels. Cuts can be made in both the $p_\perp$ of the muon relative to the calorimetric thrust axis and the jet mass of the non-muon associated jet. The jet mass, M_{jet}, is defined in terms of hemispheric thrust, $T_{1/2}$, and beam energy, E_b, as $M_{jet} = E_b(1 - T_{1/2}^2)^{1/2}$. Figure 5(a) shows the histogram for muons with $p_\perp \geq 1$ GeV/c versus the observed jet mass opposite to the recoiling muon. The theoretically calculated and absolutely normalized Monte Carlo distribution assuming only u, d, s, c, and b

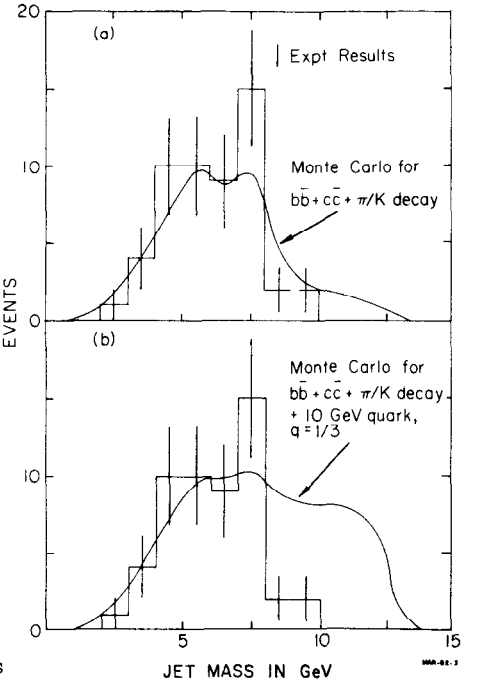

Fig. 5. The observed distribution of multihadron events containing a muon with $p_\perp > 1$ GeV/c and $p > 2$ GeV/c as a function of the mass of the "recoiling" jet in GeV. (a) Shows the observed histrogram and the absolutely normalized Monte Carlo prediction for multihadron production through standard quark flavors. (b) Shows the observed distribution and the predicted distribution for production via the standard quark flavors and an additional t quark with 1/3 charge and a mass of 10 GeV.

quarks is in excellent agreement with the observed distribution. Figure 5(b) shows the same experimental distribution compared with that expected from multihadron production based on u, d, s, c, b, and a 1/3 charged t quark of mass 10 GeV and a 10% branching ratio for decay into muons. Clearly the production of an additional 1/3 charged quark with this mass and branching ratio is ruled out by the data. Alternatively the data confirms the branching ratio into muons for the B-meson observed by the Cornell CLEO detector.

b. α_s for Flavor-Tagged Samples

Detected muons can be used to provide flavor-tagging. With cuts of $p_{\perp\mu} < 1$ GeV/c the event sample should contain 11% $b\bar{b}$, 69% $c\bar{c}$ and 20% π/K decay, and with $p_{\perp\mu} > 1$ GeV/c it should contain 44% $b\bar{b}$, 41% $c\bar{c}$ and 15% π/K decay. Multiplicity distributions were closely similar for tagged and untagged events. Energy-energy correlation measurements made on muon-tagged multihadron events shows α_s to be identical, within errors ($\sim$ 20%), to that obtained from the total multihadron sample, thus confirming the independence of α_s of quark flavor.

c. Lifetime Measurements on Muon Tagged Events

Using the displacement of the muon from the jet vertex and the displacements of the jet vertices limits on B-lifetimes have been obtained. The value is

$$\tau_b < 3.7\ 10^{-12} \text{ sec with a 95\% confidence level.}$$

5. Weak-EM Interferences

a. Muon and Tau Pair Charge-Asymmetry in Production

A total of 1,876 muon pairs suitable for charge-asymmetry measurements have been observed. The resultant charge-asymmetry $A_{\mu\mu}$ at $\sqrt{s}$ = 29 GeV is

$$A_{\mu\mu} = -0.044 \pm 0.024 \quad \text{with a } \chi^2/df = 21/18$$

and compares with -0.063 expected from the standard model.

A total of 1,247 tau pair events suitable for asymmetry measurements were observed. The measured charge-asymmetry is

$$A_{\tau\tau} = -0.013 \pm 0.029 \quad \text{with a } \chi^2/df = 22/16$$

with -0.063 expected from the standard model.

b. Bhabha Scattering

The angular distribution for Bhabha scattering has been found to be in good agreement with that predicted from theory. From the results the Weinberg-Salem angle θ_w is found to be

$$\sin^2\theta_w = 0.24 \pm 0.10$$

or

$$0.05 \leq \sin^2\theta_w \leq 0.44 \text{ with a 95\% confidence level.}$$

6. Limits for the Production of New Particles

The characteristics of our event samples are completely consistent with production of known lepton and quark flavors via one photon annihilation and two photon processes.

Table I summarizes the present status of a number of our particle searches. Method A refers to a scan of events containing one isolated muon and a jet. This event class would contain events resulting from production of a pair of heavy leptons and or supersymmetric-tau pairs, or technipions, or charged Higgs production. The jet-mass, multiplicity distribution and unbalanced momenta in the plane perpendicular to the beam have been used to provide limits for the production of these particles.

Method B uses acollinear muon pairs selected with acollinearity angles > 10^o,

TABLE I

Summary of Particle Searches

Particle	Decay Mode(s)	Method†	Mass Range Excluded	Confidence Limit
Charge 2/3 t Quark	$2t \rightarrow (\mu+Jet) + Jet$	C	3 - 13 GeV	95%
Charge 1/3 t Quark	$2t \rightarrow (\mu+Jet) + Jet$	C	5 - 12 GeV	95%
Heavy Charged Lepton	$2L \rightarrow (\mu\nu\nu) + Jet$	A	4 - 14 GeV	95%
Technipion and Charged Higgs	$2\pi^*$(or 2H) $\rightarrow$ 2(bc) Jets	C	7 - 12 GeV	95%
	$2\pi^*$(or 2H) $\rightarrow$ 2(cs) Jets	C	3 - 5 GeV and 8 - 10 GeV	95%
	$2\pi^*$(or 2H) $\rightarrow (\tau\nu) + Jet$	A	BR(H $\rightarrow \tau+\nu$) < 8% for 5 - 10 GeV	95%
Supersymmetric Muon	$\tilde{\mu} \rightarrow \mu$ + Photino	B	2 - 13 GeV	95%
Supersymmetric Tau	$\tilde{\tau} \rightarrow \tau$ + Photino	A	7 - 13 GeV	95%

†Methods A, B, and C are described in the body of the text.

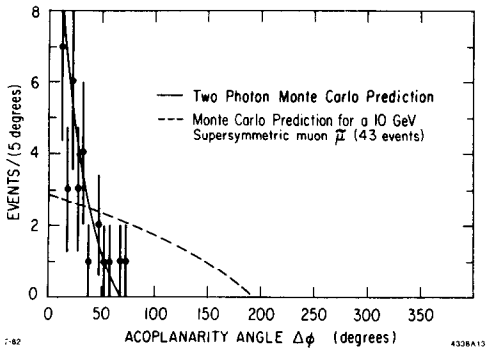

Fig. 6. The distribution of acoplanar muon pairs as a function of the acoplanarity angle. The solid curve is the Monte Carlo prediction for standard particle production, and the dashed curve is the prediction for the additional production of supersymmetric muon pairs.

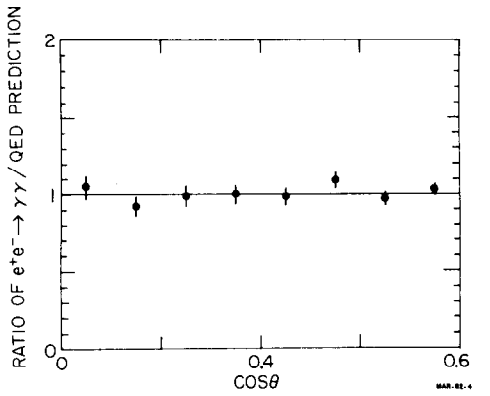

Fig. 7. The experimentally observed ratio of annihilation into two photons as a function of the cosine of the production angle, θ.

$p_\perp$ > 3 GeV, and no photon detected. 31 events were observed in 14 pb^{-1}. Figure 6 shows the observed acoplanarity distribution compared with the two photon Monte Carlo predictions. The dotted curve shows the distribution of the additional 43 events that would be expected from the production of supersymmetric-muons with masses of 10 GeV.

Method C has been described in Section 4a and obtains limits from the jet-mass distributions associated with muon-tagged multihadron events. The limits, based on analysis of these jet-mass distributions, on the production of new quark flavors, charged Higgs and technipions are tabulated under Method C in Table I.

Table I provides strong evidence against the production of new charged particle states in the PEP energy domain.

We have observed 154 $\mu^+\mu^-\gamma$ events. Their angular distribution and momentum distributions are entirely consistent with the predictions of QED, and there is no evidence for production of $\mu\mu^*$ pairs being produced. Also 17 $\mu^+\mu^-\gamma\gamma$ events have been analyzed and rule out production of excited $\mu^*\mu^*$ pairs with masses < 14 GeV.

Figure 7 shows the ratio of $e^+e^- \to \gamma\gamma$ divided by the predicted cross section versus angle. The luminosity calibrations for this measurement were based on Bhabha scattered events selected with identical criteria to the two photon annihilation events. The final results are virtually free of systematic errors and are statistics limited. With a 95% confidence level, the mass of an excited e* propagator in electron-positron annihilation into two photons is restricted to mass > 55 GeV.